Cellular Signalling 60 (2019) 114–121

Contents lists available at ScienceDirect

Cellular Signalling

journal homepage: www.elsevier.com/locate/cellsig

A fission yeast platform for heterologous expression of mammalian adenylyl cyclases and high throughput screening

Rachel A. Getz[a], Grace Kwak[a], Stacie Cornell[a], Samuel Mbugua[a], Jeremy Eberhard[a], Sheng Xiang Huang[a], Zainab Abbasi[a], Ana Santos de Medeiros[a,1], Rony Thomas[a], Brett Bukowski[a], Patricia K. Dranchak[b], James Inglese[b], Charles S. Hoffman[a,*]

[a] Biology Department, Boston College, 140 Commonwealth Ave., Chestnut Hill, MA 02467, USA
[b] National Center for Advancing Translational Sciences, National Institutes of Health, Rockville, MD 20850, USA

ARTICLE INFO

Keywords:
High-throughput screen
Adenylyl cyclase
Schizosaccharomyces pombe
Diphenyleneiodonium chloride

ABSTRACT

The fission yeast *Schizosaccharomyces pombe* uses a cAMP signaling pathway to link glucose-sensing to Protein Kinase A activity in order to regulate cell growth, sexual development, gluconeogenesis, and exit from stationary phase. We previously used a PKA-repressed *fbp1-ura4* reporter to conduct high throughput screens (HTSs) for inhibitors of heterologously-expressed mammalian cyclic nucleotide phosphodiesterases (PDEs). Here, we describe the successful expression of all ten mammalian adenylyl cyclase (AC) genes, along with the human GNAS $G\alpha_s$ gene. By measuring expression of an *fbp1-GFP* reporter together with direct measurements of intracellular cAMP levels, we can detect both basal AC activity from all ten AC genes as well as GNAS-stimulated activity from eight of the nine transmembrane ACs (tmACs; AC2-AC9). The ability to use this platform to conduct HTS for novel chemical probes that reduce PKA activity was demonstrated by a pilot screen of the LOPAC®^{1280} library, leading to the identification of diphenyleneiodonium chloride (DPI) as an inhibitor of basal AC activity. This screening technology could open the door to the development of therapeutic compounds that target GNAS or the ACs, an area in which there is significant unmet need.

1. Introduction

The budding yeast *Saccharomyces cerevisiae* and the fission yeast *Schizosaccharomyces pombe* have been premier model organisms for decades [1,2]. As single-celled eukaryotes that can be maintained as haploid or diploid cells, they are ideal for genetic screens to identify genes of interest in a wide variety of biological processes. In addition, their ability to maintain autonomously-replicating plasmids together with their highly active homologous recombination machinery have made them particularly amenable to molecular genetic approaches, including the cloning and expression of genes from other organisms.

The use of yeast in cell-based high throughput screens (HTSs) has increased in recent years [3,4], and these screens can be deployed as either growth-based or reporter-based assays. There are two advantages to yeast-based screens over mammalian/pathogen cell-based screens when targeting the activity of a specific mammalian or pathogen protein. The first is the ease and low cost of culturing yeast versus mammalian cells or pathogens. The second is the ability to construct strains that can readily distinguish hit compounds that target the foreign protein from those that target another protein that acts in the same pathway. For example, in screens that target essential proteins from a pathogen, one can construct a strain expressing the target protein and a second one expressing the human homolog as a way of counter-screening for compounds with pathogen target selectivity. Such target identification is generally more challenging when conducting pathogen or cell culture phenotypic assays [5]. While biochemically-based HTSs also effectively identify compounds that target the protein of interest, many targets, particularly membrane-associated proteins are not readily amenable to HTS-compatible biochemical assay formats [6,7] Further, these screens can result in compounds that are not cell permeable and require synthesis-intensive structural modification to produce a compound that is effective in cell culture. In contrast, hit compounds from our previous yeast-based HTS are, by definition, cell permeable and often show relevant biological activity in cell culture

* Corresponding author at: Biology Department, Boston College, 140 Commonwealth Ave., Higgins Hall Rm. 401B, Chestnut Hill, MA 02467, USA.
E-mail addresses: mbugua@bc.edu (S. Mbugua), eberharj@bc.edu (J. Eberhard), huangsi@bc.edu (S.X. Huang), abbasiz@bc.edu (Z. Abbasi), thomasry@bc.edu (R. Thomas), bukowskb@bc.edu (B. Bukowski), patricia.dranchak@nih.gov (P.K. Dranchak), jinglese@mail.nih.gov (J. Inglese), hoffmacs@bc.edu (C.S. Hoffman).
[1] Current address: Medical & Molecular Genetics, Indiana University, IN, USA.

https://doi.org/10.1016/j.cellsig.2019.04.010
Received 18 March 2019; Received in revised form 12 April 2019; Accepted 22 April 2019
Available online 24 April 2019

[8–10]. That is not to say that there are no limitations to this screening approach. While compounds that are cell permeable to yeast are very likely to be cell permeable to mammalian cells, the converse is not necessarily true, such that some compounds that would be effective in mammalian cells will not be detectable in a yeast-based assay.

3′-5′-Cyclic adenosine monophosphate (cAMP) signaling in humans and other mammals involves two large families of proteins, adenylyl cyclases (ACs) that convert ATP to cAMP and cyclic nucleotide phosphodiesterases (PDEs) that convert cAMP to 5′AMP. There are ten mammalian AC proteins. AC1 through AC9 are 12-transmembrane-domain proteins (tmACs), while sAC is a soluble protein [11,12]. The tmACs fall into four groups based on differences in regulation by G protein subunits and sensitivity to forskolin [12]. An even larger superfamily of PDEs exists in mammals, encoded by 21 genes that are grouped into 11 families [13–15]. Of these 21 genes, 16 encode PDEs that display activity against cAMP or both cAMP and cGMP. While there is a relatively large toolkit of probe compounds for PDEs that are effective in cells [13,14], the same cannot be said for compounds targeting ACs [12], partially due to the inability to take traditional biochemical approaches using purified proteins as the tmACs are integral membrane proteins.

Both budding yeast and fission yeast systems have been developed for characterizing proteins involved in cAMP signaling. In budding yeast, the human PDE4A, PDE4B and PDE7A genes, as well as the rat PDE4B gene, were cloned from cDNA libraries based on their ability to restore heat shock resistance to heat shock-sensitive strains with elevated cAMP levels due to an activated $Ras2^{val19}$ protein or deletion of the two budding yeast PDE genes [16–18]. The heat shock assay was also used to demonstrate the ability of the PDE4 inhibitor rolipram to inhibit PDE4 activity in yeast [19]. However, this assay is based on the behavior of stationary phase cells that are undoubtedly less permeable than exponentially-growing cells. Thus, 500 μM rolipram was required to restore heat shock sensitivity to PDE4-expressing strains. Similar studies in a strain expressing PDE3A required the use of PDE3 inhibitors trequensin and milronone at concentrations of 0.65 mM and 1.9 mM, respectively [20]. As such, both the high concentrations of the compounds required in these assays and the manipulations of the cells to detect the effect of the compounds make this system untenable for HTSs.

In contrast to the budding yeast system, the fission yeast platform for detecting PDE activity from heterologously-expressed genes relies on exponential phase growth and is amenable for HTSs [21]. Strains that express a PKA-repressed *fbp1-ura4* reporter [22,23] are made sensitive to the pyrimidine analog 5-fluoro-orotic acid (5FOA) by adjusting the level of endogenous cAMP production (or exogenous cAMP or cGMP supplementation of the growth medium) relative to the PDE activity so that the PKA activity is too low to repress the reporter in the absence of a PDE inhibitor [24,25]. Using this platform, we have successfully detected both known and novel PDE4, PDE5, PDE7, PDE8, and PDE11 inhibitors in a 384-well-based HTS format [8–10,25,26]. Inhibition of PDE4 activity by 2 μM rolipram can be detected by both the 5FOA growth assay and by an *fbp1-GFP* -based fluorescence assay [9,24,27–29], demonstrating the greater sensitivity of this platform as compared to the budding yeast-based detection systems.

Here, we describe a fission yeast-based platform for detecting inhibitors of mammalian ACs or the GNAS $G\alpha_S$ that stimulates the tmACs. All ten mammalian AC genes were cloned into various expression vectors, along with both wild type and mutationally-activated alleles of GNAS. Both basal and GNAS-stimulated activity of the ACs can be shown using an *fbp1-GFP* assay and by direct measurement of cAMP levels via mass spectrometry. A pilot screen of 1280 compounds from the Sigma-Aldrich LOPAC®1280 library using a strain expressing AC9 and $GNAS^{R201C}$ identified diphenyleneiodonium chloride (DPI) as a potent inhibitor of AC9 activity. Direct measurements of cAMP levels in *S. pombe* strains expressing various ACs shows that DPI displays some degree of selectivity among the mammalian ACs and acts at the level of basal AC activity.

Table 1
Mammalian AC and *GNAS* genes expressed in *S. pombe*.

Adenylyl cyclase	Organism	Reference	Promoter
AC1	*H. sapiens*	XM_005249584	*tif471*
AC2	*H. sapiens*	NM_020546.2	*adh1*
AC3	*R. norvegicus*	M55075.1	*lys7*
AC4	*R. norvegicus*	M80633.1	*adh1*
AC5	*C. lupis*	NP_001161932.1	*tif471*
AC6	*C. lupis*	NM_001195147.1	*lys7*
AC7	*H. sapiens*	NM_001114.4	*adh1*
AC8	*R. norvegicus*	NM_017142.1	*tif471*
AC9	*H. sapiens*	NM_001116.3	*tif471*
sACt (aa 1–469)*	*R. norvegicus*	NM_021684.1	*lys7*
GNAS			
$GNAS^+$	*H. sapiens*	NP_000507.1	*nmt1*
$GNAS^{R201C}$	*H. sapiens*	NP_000507.1	*nmt1*
$GNAS^+$	*H. sapiens*	NP_000507.1	*adh1*
$GNAS^{R201C}$	*H. sapiens*	NP_000507.1	*adh1*
PDE			
PDE4D2	*H. sapiens*	AF012074.1	*cgs2*
PDE4D3	*H. sapiens*	U50159.1	*cgs2*
PDE7A1	*H. sapiens*	NM_002603	*cgs2*

Mammalian AC or *GNAS* genes were cloned by gap repair transformation into linearized expression vectors containing the *nmt1*, *adh1*, *tif471*, or *lys7* promoters. After DNA sequencing to confirm that the genes were free of PCR-generated mutations, the plasmids were linearized at a site that is also present in the *S. pombe* genome and used to transform an *S. pombe* strain to leucine- or lysine-prototrophy. Transformants carrying a copy of the plasmid integrated in the genome were identified so as to reduce the copy number of the cloned genes, reduce cell to cell variability, and maintain mitotic stability. Mammalian PDE genes were directly integrated into the *S. pombe cgs2* (PDE) locus.

* sACt represents a truncated form of the soluble AC that possesses the catalytic domain, but not the inhibitory regulatory domain [35].

2. Materials and methods

2.1. Yeast strains, media, and growth conditions

The genotypes of *S. pombe* strains used in this study are presented in Supplemental Table 1. Cells were cultured at 30 °C in YES-rich (yeast extract medium with supplements), EMM (Edinburgh Minimal Medium), or 5FOA media as described previously [22,30,31]. Cloning of mammalian PDE genes *PDE4D2*, *PDE4D3*, and *PDE7A1* (Table 1) and insertion into the *S. pombe* $cgs2^+$ (PDE) locus as well as the $fbp1\text{-}ura4^+$ and *fbp1-GFP* reporters have been previously described [9,22,25,29].

2.2. Cloning of mammalian AC and GNAS genes into yeast expression vectors

Mammalian AC genes were cloned into *S. pombe* expression vector pJV1 [28], allowing expression from either the weak *lys7* promoter or the moderately-active *tif471* promoter, or pLEV3 [32], allowing expression from the moderately-active *adh1* promoter (Table 1). All strains expressing mammalian ACs lacked *S. pombe* AC activity (*git2-2*), while all strains expressing mammalian PDEs lacked *S. pombe* PDE activity (*cgs2-2*). Cloning was carried out by gap repair transformation in which the gene of interest was PCR-amplified using oligonucleotides possessing 45 to 60 base pairs of homology to the expression vector at sites flanking a unique restriction enzyme site in the vector [2]. Template DNAs for PCR reactions were plasmids generously provided by researchers in the AC community, or, in the case of AC9, a human skeletal muscle cDNA library. Host fission yeast strains lacked endogenous AC activity (*git2-2*; [33]) and PDE activity (*cgs2-2*; [34]) and expressed a PKA-repressed *fbp1-GFP* reporter gene [29]. As such, the acquisition of a functional AC could be readily detected by a change in

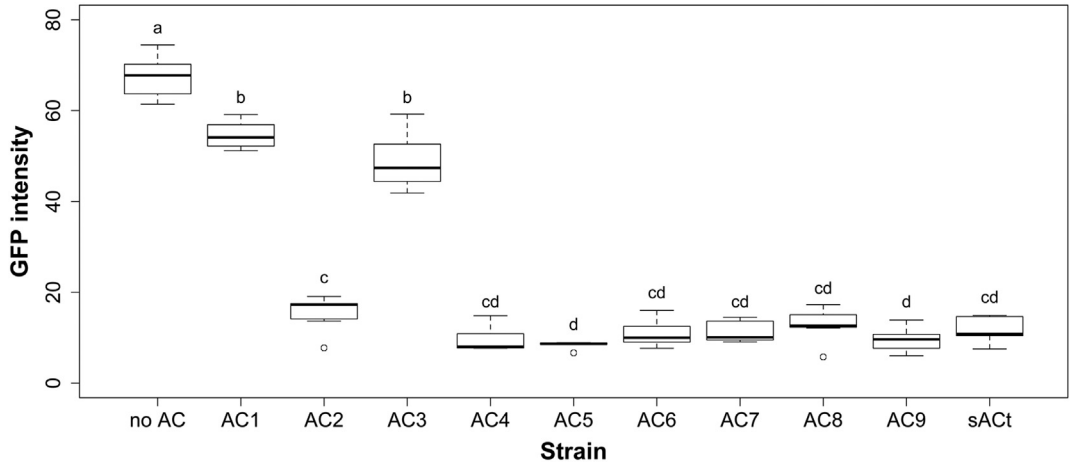

Fig. 1. Basal activities of mammalian ACs reduce *fbp1-GFP* expression in strains lacking PDE activity. Basal AC activity was assessed by growing strains to exponential phase and measuring the GFP signal (excitation 488, emission 509) and absorbance (OD_{600} to assess cell density) of cells transferred to triplicate wells of a 384 microtiter dish. GFP values were normalized by dividing the fluorescence by the absorbance of each well. Data were subjected to an ANOVA with a post-hoc Tukey's HSD test. Letters above each strain denote categories with statistically significant differences. Strains (all *cgs2–2* mutants, thus lacking PDE activity) used were CHP1652 (no AC), CHP1845 (AC1), CHP2016 (AC2), CHP1989 (AC3), CHP1812 (AC4), CHP1851 (AC5), CHP1981 (AC6), CHP1813 (AC7), CHP2015 (AC8), CHP2024 (AC9), and CHP2017 (sACt). Significant differences among strains were detected (ANOVA, $F_{10,70} = 283.7$, $p < .0001$), with AC-expressing strains displaying significantly lower GFP levels than CHP1652 (no AC control), consistent with having higher PKA activity due to AC activity.

growth rate, cell.

length during cytokinesis, and GFP expression [29]. These clones were then rescued into *E. coli* for plasmid isolation and DNA sequence analysis. Clones possessing wild type AC sequences were linearized at a unique site to target their integration into the *S. pombe* genome by homologous recombination at either the *adh1* locus (for pLEV3 derivatives) or the *lys2* locus (for pJV1 derivatives). The wild type human GNAS gene and the mutationally activated $GNAS^{R201C}$ gene were cloned into expression vectors pNMT1 and pLEV3 (Table 1), and integrated into the *ars1* locus by homologous insertion of *Blp*I- linearized plasmids.

2.3. Small molecules

Diphenyleneiodonium chloride was purchased from Sigma-Aldrich (D2926), (R,S) Rolipram was purchased from AG Scientific (R-1012) and BC54 was purchased from ChemDiv (C098-0484).

2.4. GFP assays

GFP assays to characterize mammalian AC activity were carried out using strains that express the PKA-repressed *fbp1-GFP* reporter (Supplemental Table 1) [29]. Basal GFP expression was determined by growing cultures to exponential phase (~10^7 cells/ml) in EMM medium containing leucine, lysine, histidine, adenine and uracil (EMM complete). 50 µl of cell culture was pipetted into three wells of a 384-well black wall, clear bottom microtiter dish. Cells were allowed to settle for 90 min before reading GFP (excitation 488, emission 509) and OD_{600} (to normalize to cell density) using a SpectraMax M5 plate reader. Five to ten independent assays were performed for each strain.

2.5. High-throughput screens (HTSs)

A quantitative HTS (qHTS; [36]) of the Sigma-Aldrich LOPAC®^{1280} chemical library was carried out at the NCATS screening facility. Strain CHP2027, expressing human AC9, $GNAS^{R201C}$ and PDE4D2, was grown to exponential phase in EMM complete liquid medium and diluted to 5×10^6 cells/ml. Assays were carried out in 1536-well Aurora black wall, clear bottom, low base plates. Two microliters EMM complete medium was added to all wells using a Combi liquid handler. Subsequently, 23 nl compounds were added by Pintool, followed by 2 µl of cells by Combi. Evaporation was prevented by covering plates with metal lids containing holes to allow gas diffusion. Plates were incubated at 30 °C for 18 h and the fluorescent signal was read using an Acumen laser cytometer, gated to avoid detection of soluble fluorescent compounds. The library was contained in seven plates representing a 1:2 titration (three-fold dilutions) from 10 mM to 13.7 µM (final concentrations of ~57 µM to 78.4 nM). Z' factors ranged from 0.49 to 0.63, indicating that this is a robust assay suitable for HTS [37]. Compounds were assigned to class curves based on efficacy and the identification of upper and lower asymptotes [36]. Further characterization of the DPI compound was carried out using a freshly-made solution and a 16 point 2:1 titration from 10 mM to 22.8 µM. Activity was normalized to a control of 6.3 µM DPI final concentration as this was the most effective concentration in the original library screen.

2.6. cAMP assays

Strains were grown to exponential phase in EMM complete liquid medium. After treatment with compounds as described in the relevant experiments, cells were collected by filtration over glass fiber filters and immersed in 1 ml 1 M formic acid to release cAMP. 400 µl of the solution was dried in a Speedvac and resuspended in 200 µl water. cAMP levels were measured on an Agilent 6460 Triple Quad Mass Spectrometer as previously described [38].

2.7. Statistical analyses

GFP intensity differences among strains in Fig. 1 were tested with an analysis of variance (ANOVA), and a post-hoc Tukey's Honest Significant Differences (Tukey's HSD) test to determine which strains are significantly different from each other. Both analyses were conducted using R v3.5 (www.r-project.org). Student *t*-tests were used to analyze data from strains with and without GNAS for Fig. 2, strains expressing wild type GNAS versus mutationally-activated $GNAS^{R201C}$ for Fig. 4, and DMSO-treated cells versus DPI-treated cells for Fig. 7. *P* values are presented in the figures and figure legends.

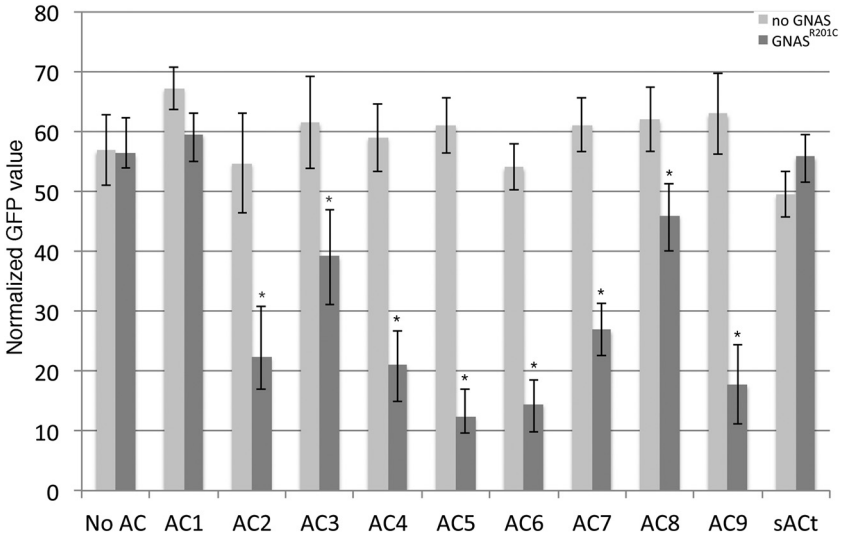

Fig. 2. *fbp1-GFP* expression in strains expressing mammalian ACs together with PDE4D in the presence or absence of $GNAS^{R201C}$. GNAS-mediated stimulation of mammalian ACs was examined by *fbp1-GFP* expression in strains expressing the highly-active cAMP PDE PDE4D2 (with the exception of AC1 strains that expresses the less active PDE4D3 in an attempt to sensitize the strain to detect GNAS-mediated AC stimulation), which lowers PKA activity in the absence of GNAS-mediated AC stimulation. Normalized GFP values were determined as described in Fig. 1. Strains used were as follows (each pair represents the strain lacking GNAS followed by the $GNAS^{R201C}$ strain): no AC (CHP1643, CHP1797), AC1 (CHP1911, CHP1884), AC2 (CHP1920, CHP1923), AC3 (CHP1976, CHP1977), AC4 (CHP2009, CHP1826), AC5 (CHP1853, CHP1852), AC6 (CHP1960, CHP1963), AC7 (CHP1829, CHP1817), AC8 (CHP2011, CHP2013), AC9 (CHP2026, CHP2027), and sACt (CHP1972, CHP1971). *-P value < .0001 compared to strain containing the same AC, but lacking GNAS.

3. Results

3.1. Construction of a strain collection expressing mammalian ACs and GNAS in S. pombe

As described in the Materials and Methods section, all the mammalian AC genes, as well as both wild type GNAS and mutationally activated $GNAS^{R201C}$ genes were initially cloned by gap repair transformation into autonomously-replicating plasmids. Once the DNA sequence analyses confirmed the absence of PCR-generated mutations, each plasmid was linearized and used to transform yeast strains, and transformants carrying a copy of the plasmid integrated by homologous recombination into the yeast genome were identified. Subsequent crosses were used to create a collection of strains expressing these ACs in the presence or absence of GNAS, as well as the presence or absence of a PDE [25]. This strain collection was then used to examine both basal and GNAS-stimulated AC activity and to develop an effective HTS for compounds that lower cAMP levels by either inhibiting the AC or GNAS or by stimulating the PDE in a given strain.

3.2. Detection of basal and GNAS-stimulated AC activity using a PKA-repressed GFP reporter

Two sets of strains were characterized using a GFP assay carried out in a 384-well microtiter dish format (see Materials and Methods). All strains carry a partial deletion of the coding region for the catalytic domain of the *S. pombe git2/cyr1* AC gene (*git2-2* [33]).The first set of strains lack PDE activity, carrying a frameshift mutation in the *S. pombe cgs2* PDE gene (*cgs2-2*; [31,34]). There were significant differences in the GFP signals among strains (Fig. 1; ANOVA, $F_{10,70} = 283.7$, $p < .0001$). A Tukey's HSD test showed that all AC-expressing strains had significantly lower values than the no AC control (Fig. 1). Strains expressing AC1 and AC3 had intermediate GFP values that were significantly higher than the other AC-expressing strains, while the AC2-expressing strain had a significantly higher value than strains expressing AC5 and AC9.

The second set of strains express the highly-active human PDE4D2 cAMP-hydrolyzing PDE (with the exception of the AC1-expressing strains that express the less active PDE4D3 enzyme) together with each of the ACs in the presence or absence of the mutationally-activated human $GNAS^{R201C}$ $G\alpha_S$. As seen in Fig. 2, the basal tmAC activity (i.e., strains lacking GNAS) is insufficient to lower GFP levels when compared to a strain lacking AC activity. The strain expressing the sACt enzyme in the absence of GNAS does display a modest, but statistically-significant reduction in the GFP signal ($p < .01$), however the sACt strain expressing $GNAS^{R201C}$ does not show a similar reduction, consistent with the enzyme not being regulated by GNAS [11]. Strains expressing AC2 through AC9 show a significant decrease in the GFP signal upon the addition of $GNAS^{R201C}$, demonstrating our ability to detect GNAS- mediated stimulation of these eight tmACs. While there may be a slight reduction in the GFP signal in the AC1-expressing strain relative to the AC1 strain lacking GNAS, it is not statistically significant.

3.3. GNAS-mediated stimulation of AC9 via direct measurement of cAMP

To develop a more direct assessment of AC activity, GNAS-mediated AC stimulation, and the effect of small molecules AC activity, we investigated our ability to measure cAMP levels in these strains by mass spectrometry. While the GFP assays readily demonstrate GNAS-mediated activation of AC2-AC9, we observed that cAMP levels were barely detectable due to the activity of the co-expressed PDE (data not shown). We therefore examined the effect of the PDE4 inhibitor rolipram on cAMP levels over time.

We observed that cAMP levels dramatically rise after rolipram addition (40 μM final concentration), with a majority of the response seen within 60–90 min (Fig. 3).

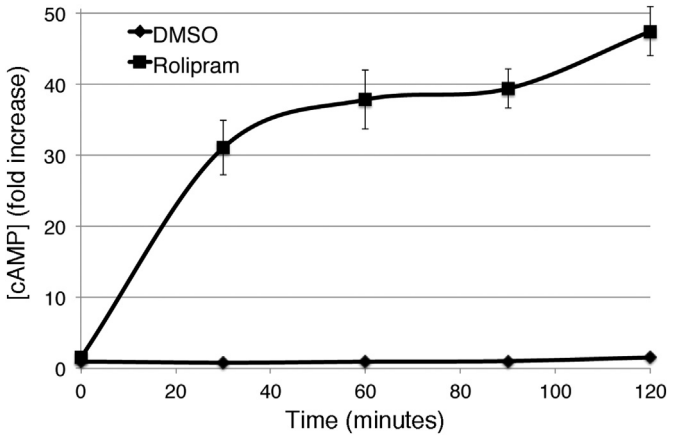

Fig. 3. cAMP accumulation in response to rolipram inhibition of PDE4D2. An exponential phase culture of strain CHP2027 (AC9 $GNAS^{R201C}$ PDE4D2) was treated with either 40 μM rolipram or an equivalent volume of DMSO (vehicle control) and grown at 30 °C. At the indicated times, 5 ml cultures were collected and cAMP was extracted and measured by mass spectrometry (see Materials and Methods). cAMP levels are presented as a fold increase from the zero timepoint measurements.

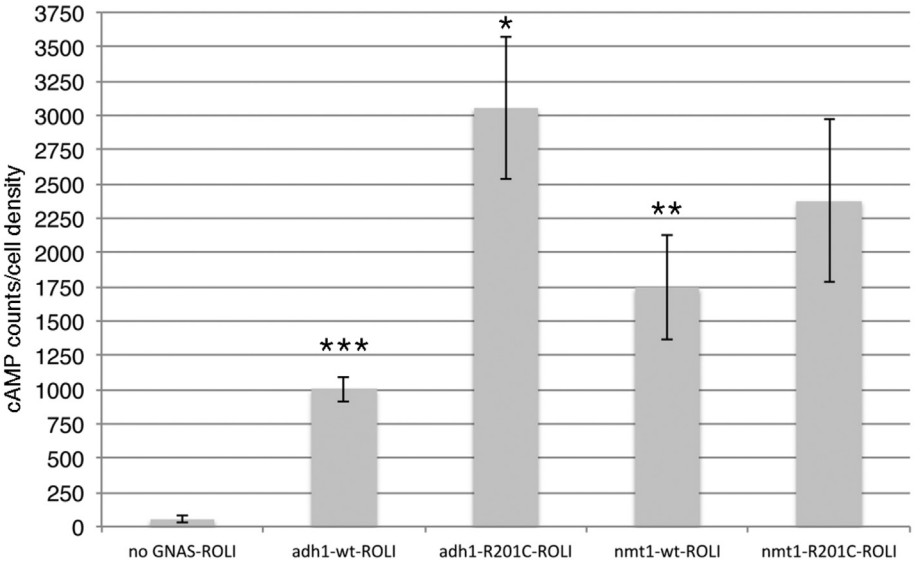

Fig. 4. cAMP levels in AC9 strains expressing either no GNAS, wild type GNAS or GNAS^{R201C}. Cultures of strains CHP2026 (AC9 PDE4D2), CHP2213 (AC9 *adh1*-wtGNAS PDE4D2), CHP2214 (AC9 *adh1*-GNAS^{R201C} PDE4D2), CHP2330 (AC9 *nmt1*-wtGNAS PDE4D2), and CHP2027 (AC9 *nmt1*- GNAS^{R201C} PDE4D2) were grown to exponential phase and treated with 40 μM rolipram (to inhibit PDE4D2) for 60 min before collecting cells to make cAMP extracts. cAMP levels were normalized to the cell density of each culture. Values represent mean and standard deviations for three independent assays. *- *P* value < .01 compared to strain expressing wtGNAS from *adh1* promoter. **- *P* value < .001 compared to strain lacking GNAS. ***- P value < .0001 compared to strain lacking GNAS.

To assess the effect of expressing either the wild type GNAS (wtGNAS) or the mutationally-activated GNAS^{R201C} on AC9 activity, we measured cAMP levels in strains after a one-hour exposure to rolipram and normalized cAMP levels to cell density of the cultures. As seen in Fig. 4, co-expressing GNAS with AC9 dramatically elevates cAMP levels, and that GNAS^{R201C} is significantly more effective than the wild type GNAS. The higher cAMP level observed in the strain expressing wild type GNAS from the *nmt1* promoter as compared to the strain expressing wild type GNAS from the *adh1* promoter is consistent with relative strengths of these two promoters [39].

3.4. Pilot GFP qHTS screen

To assess the ability to use the *fbp1-GFP* reporter as a read out for a HTS, we carried out a pilot qHTS using a seven point titration of the LOPAC®^{1280} library in 1536-well microtiter plates. This screen identified diphenyleneiodonium chloride (DPI) as the most effective candidate (data not shown). DPI was re-purchased and a freshly-made solution was further characterized in a 16 point titration. Activity was assessed against what had been seen as the peak activity of 6.3 μM in the screening the original LOPAC®^{1280} library plates (Fig. 5). In assays using the fresh stock of DPI, peak activity was observed at ~1.5 μM, indicating a loss of activity in the library plates. In Fig. 5A, the reduction in the GFP signal at elevated concentrations is due to toxicity. This is independent of AC inhibition as we observe a reduction in growth in all *S. pombe* strains exposed to > 2 μM DPI, including the prototrophic wild type strain 972 and growth inhibition cannot be restored by treatment of cells with exogenous cAMP plus rolipram (to inhibit PDE4D2 in tmAC-expressing strains), which would independently activate PKA ([30]; Fig. 5B).

While transcription from the *S. pombe fbp1* promoter, which is driving GFP expression in this screen, is fully derepressed within 1 h of glucose starvation in wild type cells [40], the microtiter plates were examined after 18 h to account for the suboptimal.

growth conditions. To examine the effect of DPI on cells growing in liquid culture with aeration, strains CHP2027 (AC9, GNAS^{R201C}, PDE4D2) and CHP1963 (AC6,

GNAS^{R201C}, PDE4D2) were exposed to either 2 μM DPI or an equivalent volume of DMSO and grown with aeration for 4 h before examination by microscopy. As seen.

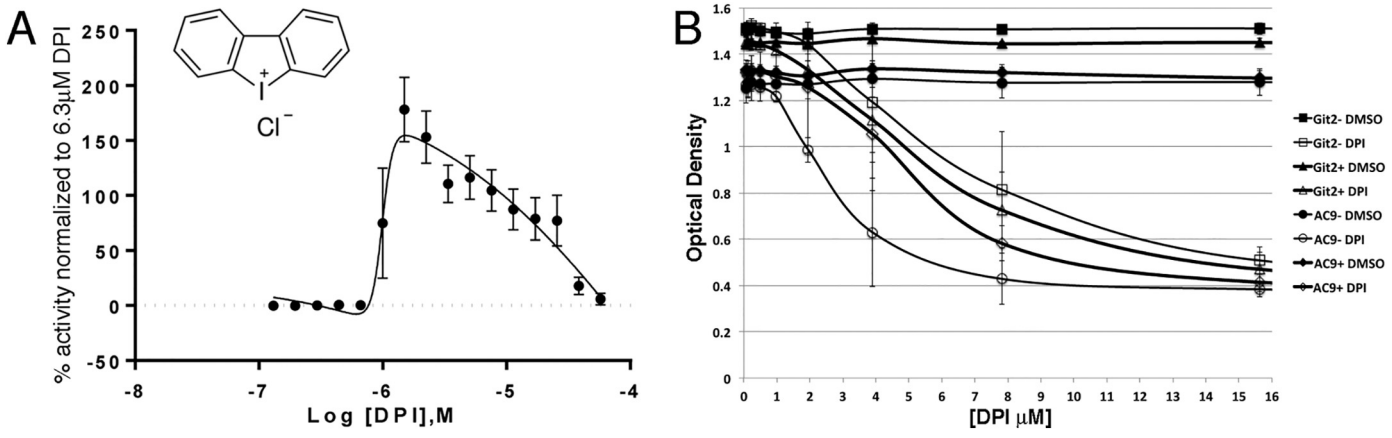

Fig. 5. Response profile of DPI for *fbp1-GFP* expression in CHP2027 (AC9 GNAS^{R201C} PDE4D2) cells and DPI toxicity test. A) Percent activity is relative to treatment with 6.3 μM DPI as this had been the peak concentration for DPI activity in the LOPAC®^{1280} library plates. Peak activity for the freshly-made solution of DPI is ~1.5 μM. Values represent means and standard deviations (n = 18). These data were refit in Prism 7.0 (GraphPad, La Jolla, CA) with nonlinear regression log (agonist) vs. response – variable slope (four parameters) fit. B) Strains CHP2027 (AC9) and 972 (Git2; h^- wild type *S. pombe* strain; [2]) were grown to exponential phase. 40 ml cultures were diluted to 2.5 × 10^6 cells/ml in either EMM with no cAMP (−) or EMM + 5 mM cAMP + 10 μM Rolipram (+) and treated with varying concentrations of DPI or an equivalent volume of DMSO and grown an additional 22 h at 30 °C before measuring optical densities. Values represent averages and SD of OD_{600} values for four independent cultures.

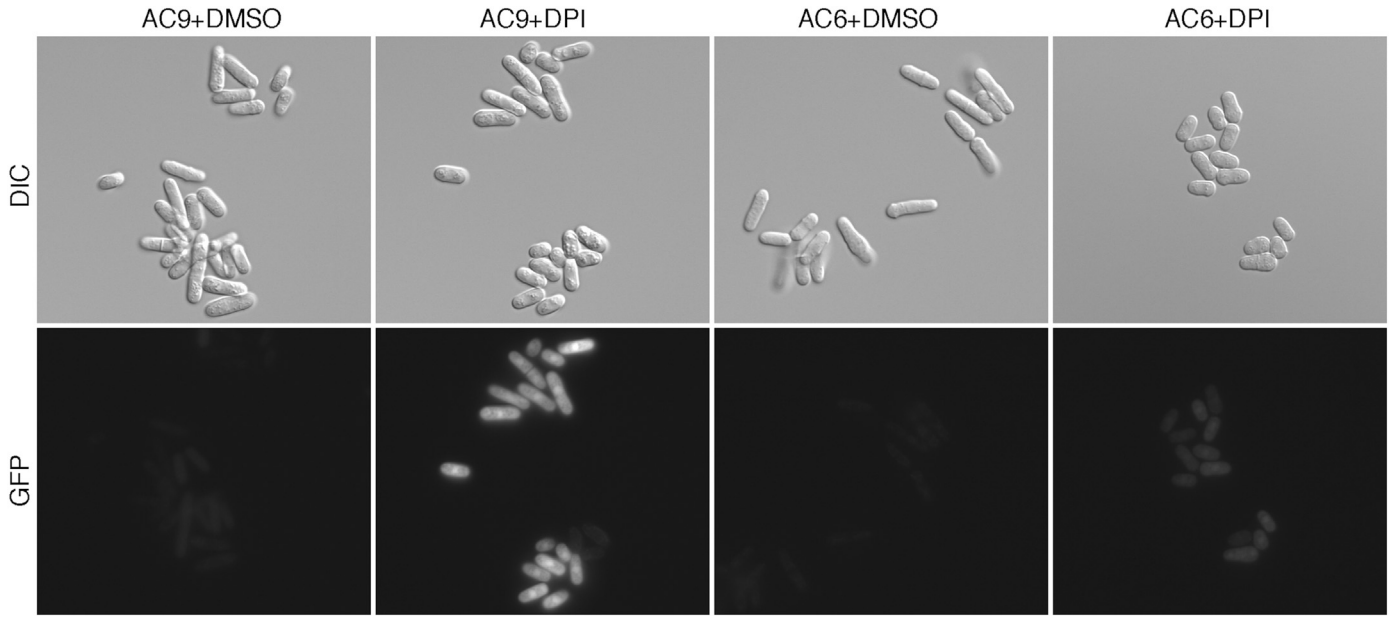

Fig. 6. DPI induction of *fbp1-GFP* expression in AC9- versus AC6-expressing strains. Strains CHP2027 (AC9 GNAS^{R201C} PDE4D2; four images on the left) and CHP1963 (AC6 GNAS^{R201C} PDE4D2; four images on the right) cells were grown to exponential phase in EMM complete liquid medium and used to make 2 ml cultures diluted to 4 × 10^6 cells/ml. These cultures were treated with either 2 µl 2 mM DPI or 2 µl DMSO and grown for an additional 4 h. Cells were imaged using an Axioplan 2 microscope with a 40× oil objective by DIC or fluorescent microscopy. Exposure times (100 msec for DIC, 250 msec for FITC channel) were kept constant for the two strains. The AC9-expressing strain shows a dramatic elevation in GFP expression in response to DPI, while the AC6-expressing strain shows only a slight elevation in the GFP signal.

in Fig. 6, DPI treatment significantly increases the GFP signal in cells expressing AC9, but has only a modest effect on the GFP signal in cells expressing AC6. This differential effect argues against the idea that the fluorescent signal is an artifact that is unrelated to *fbp1-GFP* expression.

3.5. DPI lowers cAMP levels in strains expressing mammalian ACs

cAMP assays were carried out to determine whether or not DPI treatment of strains expressing various ACs lowers cAMP levels. Strains expressing either the *S. pombe* Git2/Cyr1 AC (possessing an activated Gpa2^{R176H}*S. pombe* Gα) or GNAS^{R201C} together with AC2, AC4, AC5, AC6, AC7 or AC9 were treated with 2 µM DPI (or with DMSO as a vehicle control) for 30 min followed by 40 µM rolipram for 90 min. cAMP levels from the DPI-treated cells are presented as a percent of the DMSO controls (Fig. 7). In addition, cells expressing AC9 from an autonomously-replicating plasmid, but lacking GNAS, were also tested to determine whether or not DPI acts on basal AC activity as opposed to preventing GNAS-mediated stimulation of AC activity (Fig. 7; AC9 basal). DPI significantly lowered cAMP levels in all strains with the exception of the Git2 AC and the AC6 strains. These data suggest that DPI acts to reduce basal AC activity and that it is a fairly nonspecific inhibitor of mammalian ACs.

4. Discussion

In this study, we have laid the foundation for using fission yeast as an expression platform for proteins involved in cAMP synthesis. By adjusting cAMP hydrolysis via the removal of endogenous PDE activity

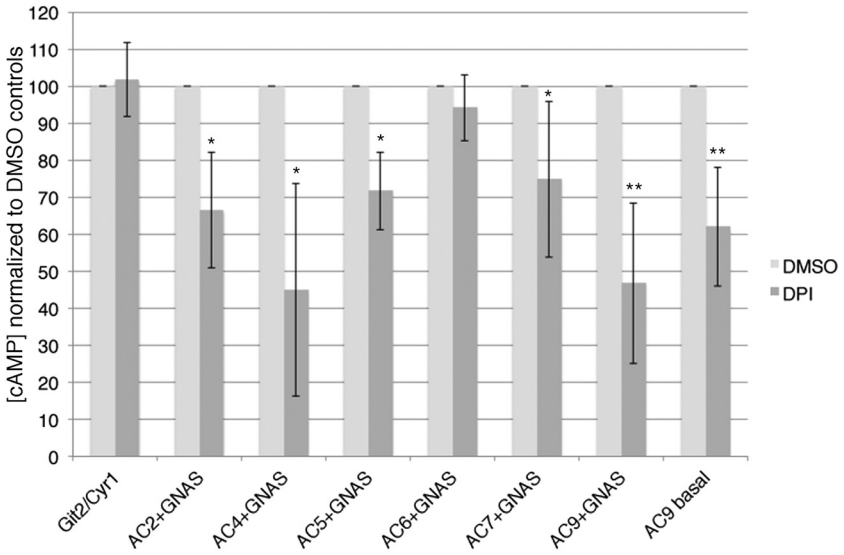

Fig. 7. Profiling of DPI effect on cAMP levels in strains expressing various ACs. Strains CHP1359 (*git2*$^+$ *gpa2*^{R176H} PDE7A), CHP1923 (AC2 GNAS^{R201C} PDE4D2), CHP1826 (AC4 GNAS^{R201C} PDE4D2), CHP1852 (AC5 GNAS^{R201C} PDE4D2), CHP1963 (AC6 GNAS^{R201C} PDE4D2), CHP1817 (AC7 GNAS^{R201C} PDE4D2), CHP2027 (AC9 GNAS^{R201C} PDE4D2), and CHP2018/pJV1-AC9 (PDE4D2/multicopy plasmid expressing AC9 for basal activity) were grown to exponential phase in EMM complete liquid medium (EMM minus lysine for CHP2018/pJV1-AC9 to maintain selective pressure for the pJV1-AC9 plasmid). Cultures were split into two samples and treated with either 2 µM DPI (final concentration) or an equivalent volume of DMSO and grown for 30 min before adding 40 µM rolipram (for CHP1359, 40 µM BC54 was added to inhibit PDE7A) and grown for an additional 90 min. cAMP extracts were made as described in the Materials and Methods. cAMP levels were determined by mass spectrometry. Values are normalized to the DMSO controls and presented as mean and standard deviation from three to six independent assays. *- P value < .05 compared to the effect of DPI on the Git2/Cyr1-expressing strain. ** P value < .01 compared to the effect of DPI on the Git2/Cyr1-expressing strain.

or the inclusion of PDEs of varying activities, we can use the PKA-repressed *fbp1-GFP* reporter to detect both basal and GNAS-mediated activated AC activity (Figs. 1 and 2; with the exception of GNAS-mediated AC1 activity; Fig. 2). In a previous study involving the expression of mammalian ACs in budding yeast, Haney and co-workers could detect GNAS-stimulated activity, but not basal activity [41], by the restoration of growth to an AC mutant strain. Similarly, most research on ACs in mammalian cell culture relies on stimulation of ACs to assess activity. As such, our fission yeast system is unique in its ability to examine both basal activity and GNAS-stimulated activity of mammalian tmACs. The one limitation here is the relatively weak activity seen for AC1 in both the presence and absence of GNAS (Figs. 1 and 2). This was observed with clones expressing AC1 from both the *adh1* and the *tif471* promoters (data not shown). The reason for this low activity is unknown.

GNAS-mediated stimulation of the tmACs can be detected both via expression of the *fbp1-GFP* reporter (Fig. 2) and by direct measurement of cAMP levels (Fig. 4). While it may seem surprising that expression of the wild type GNAS protein in the absence of an associated GPCR or Gβγ dimer also stimulates AC activity, this is consistent with our previous studies of the *S. pombe* cAMP pathway that also includes a heterotrimeric G protein in which the Gpa2 Gα directly binds and stimulates the Git2 AC [42]. Plasmid-based overexpression of the *gpa2* gene bypasses the loss of the Git3 GPCR, the Git5 Gβ or the G11 Gγ to restore repression of *fbp1* transcription [43–45]. It was only after identifying a sufficiently low level of expression that mutationally-activated alleles of *gpa2* would be distinguished from the wild type allele in this system [46]. Consistent with these data, we see a greater differential in AC9 activation by $GNAS^{R201C}$ relative to wild type GNAS when these proteins are expressed from the weaker *adh1* promoter than from the stronger *nmt1* promoter ([39]; Fig. 4).

Along with our ability to detect AC activity, the *fbp1-GFP* reporter allows for a robust HTS as demonstrated by our pilot screen of the $LOPAC^{®1280}$ library, leading to the identification of DPI as an inhibitor of basal AC9 activity (Figs. 5 and 7). This screen was carried out in 1536-well microtiter plates, allowing for the possibility of future ultra-high throughput screens, as well as qHTS screens of large libraries. To our knowledge, most yeast-based HTSs have been performed in 384-well microtiter plates, with only a couple screens done at this higher density [47,48]. In contrast to these previous screens that detected compounds based on their ability to inhibit cell growth, our screen detects a biological response via reporter gene expression, thus expanding the utility of yeast-based small molecule screening methods in a 1536-well format. As previously noted, yeast-based screens combine the strength of biochemical screens for the ability to confirm target identity with phenotypic screens for compounds that are biologically-active [3,4]. As we observed that the DPI-stimulated GFP signal remained stable between 17 and 24 h after incubation (data not shown), we could potentially screen > 80,000 compound wells/day using this assay.

We expected four possible mechanisms (other than off target activities) by which a compound might lower cAMP levels to produce an increase in *fbp1-GFP* expression. It could bind and inhibit the AC, bind and inhibit GNAS, bind the AC and inhibit the GNAS interaction with the AC, or stimulate the PDE. Following the detection of DPI as an active compound in the screen using a strain expressing AC9, $GNAS^{R201C}$, and PDE4D2, subsequent characterization suggests that DPI acts as an inhibitor of basal AC9 activity. The relatively weak effect DPI has on the AC6-expressing strain (Figs. 6 and 7) suggests that it is not working via binding GNAS. Furthermore, it does not appear to be a PDE4 activator as the cAMP measurements are performed on cells that have been exposed to the PDE4 inhibitor rolipram (Fig. 7), and we have seen DPI act on cells that express a variety of PDEs (data not shown). While we cannot fully rule out the possibility that DPI binds AC9 to reduce basal activity and to prevent GNAS from binding AC9, it is clear that DPI does reduce basal AC9 activity (Fig. 7). As such, this identification of a basal AC inhibitor is unique in the relatively nascent field of AC inhibitor discovery and development [12]. Several activities have been attributed to DPI, some mediated by membrane-associated proteins (e.g., NADH oxidase; [49,50]) consistent with the lipophilic nature (cLog P 3.80–2.77) of the compound (Fig. 5). Furthermore, the combined cationic and lipophilic properties of DPI likely result in accumulation proximal to the phospholipid head groups, possibly affecting membrane fluidity. Alterations in the lipid bilayer composition could underlie the broad perturbations on tmACs, but not the *S. pombe* AC, which it is not an integral membrane protein. DPI has also been described as an inhibitor of endothelial NOS (eNOS; [51]). However, since eNOS is activated by PKA [52], it is possible that its effect on eNOS is via AC inhibition that reduces PKA activity. Paradoxically, DPI was identified as an agonist of the GPR3 G protein coupled receptor and was shown to elevate cAMP levels in cells expressing GPR3 [53]. This result is not necessarily inconsistent with our data as we observe that some ACs, such as AC6, are relatively insensitive to DPI (Fig. 7), and may therefore be the AC activated by signaling through GPR3.

Finally, along with the ability to detect AC inhibitors, we are in a position to go on to detect mutant alleles of ACs that confer reduced sensitivity, if not full resistance, to an inhibitor as we previously did with the PDE4/7 inhibitor BC54 [9]. Such a mutation could be detected using the same criterion applied to detect functional AC clones during the construction of this strain collection. By mutagenizing an AC clone, we could introduce the population of clones into a homothallic strain that lacks endogenous AC activity and screen for transformants that retain the ability to grow in the presence of the inhibitor in question (as inhibition would lower PKA activity and shift the cells from mitotic growth to conjugation and meiosis). The identification of such mutations could play an important role in the future development of effective therapeutic compounds that target ACs as this might identify the site of action of the inhibitor and facilitate rationale drug design. The suitability of this platform to both chemical genetics and molecular genetics demonstrates the potential for future AC-targeting compound discovery and drug development.

Supplementary data to this article can be found online at https://doi.org/10.1016/j.cellsig.2019.04.010.

Acknowledgments

We thank Carmen Dessauer, Val Watts, Dermot Cooper, Tom Rich, and Sarah Sayner for AC clones, Michael Collins for GNAS clones, and Cecilia Ostlund and Howard Worman for the human skeletal muscle cDNA library used to clone the ADCY9 gene. We also thank Marek Domin for his support of the cAMP measurements via mass spectrometry and Jeffrey DaCosta for his support with regard to statistical analyses. This work was supported by the Peter Rieser Lectureship Fund (C.S.H.) and by the intramural program of NCATS, National Institutes of Health, project 1ZIATR000053-04 (J.I.).

References

[1] A.A. Duina, M.E. Miller, J.B. Keeney, Budding yeast for budding geneticists: a primer on the *Saccharomyces cerevisiae* model system, Genetics 197 (1) (2014) 33–48.
[2] C.S. Hoffman, V. Wood, P.A. Fantes, An ancient yeast for young geneticists: a primer on the Schizosaccharomyces pombe model system, Genetics 201 (2) (2015) 403–423.
[3] P.W. Denny, P.G. Steel, Yeast as a potential vehicle for neglected tropical disease drug discovery, J. Biomol. Screen. 20 (1) (2015) 56–63.
[4] P.W. Denny, Yeast: bridging the gap between phenotypic and biochemical assays for high-throughput screening, Exp. Opin. Drug. Discov. (2018) 1–8.
[5] M. Schenone, V. Dancik, B.K. Wagner, P.A. Clemons, Target identification and mechanism of action in chemical biology and drug discovery, Nat. Chem. Biol. 9 (4) (2013) 232–240.
[6] L. Tiefenauer, S. Demarche, Challenges in the development of functional assays of membrane proteins, Materials 5 (11) (2012) 2205–2242.
[7] J. Inglese, R.L. Johnson, A. Simeonov, M. Xia, W. Zheng, C.P. Austin, D.S. Auld, High-throughput screening assays for the identification of chemical probes, Nat. Chem. Biol. 3 (8) (2007) 466–479.

[8] O. Ceyhan, K. Birsoy, C.S. Hoffman, Identification of biologically active PDE11-selective inhibitors using a yeast-based high-throughput screen, Chem. Biol. 19 (1) (2012) 155–163.

[9] A.S. de Medeiros, A.R. Wyman, M.A. Alaamery, C. Allain, F.D. Ivey, L. Wang, H. Le, J.P. Morken, A. Habara, C. Le, S. Cui, A. Lerner, C.S. Hoffman, Identification and characterization of a potent and biologically-active PDE4/7 inhibitor via fission yeast-based assays, Cell. Signal. 40 (2017) 73–80.

[10] D. Demirbas, A.R. Wyman, M. Shimizu-Albergine, O. Cakici, J.A. Beavo, C.S. Hoffman, A yeast-based chemical screen identifies a PDE inhibitor that elevates Steroidogenesis in mouse Leydig cells via PDE8 and PDE4 inhibition, PLoS ONE 8 (8) (2013) e71279.

[11] M. Kamenetsky, S. Middelhaufe, E.M. Bank, L.R. Levin, J. Buck, C. Steegborn, Molecular details of cAMP generation in mammalian cells: a tale of two systems, J. Mol. Biol. 362 (4) (2006) 623–639.

[12] C.W. Dessauer, V.J. Watts, R.S. Ostrom, M. Conti, S. Dove, R. Seifert, International Union of Basic and Clinical Pharmacology. CI. Structures and small molecule modulators of mammalian adenylyl Cyclases, Pharmacol. Rev. 69 (2) (2017) 93–139.

[13] A.T. Bender, J.A. Beavo, Cyclic nucleotide phosphodiesterases: molecular regulation to clinical use, Pharmacol. Rev. 58 (3) (2006) 488–520.

[14] D.H. Maurice, H. Ke, F. Ahmad, Y. Wang, J. Chung, V.C. Manganiello, Advances in targeting cyclic nucleotide phosphodiesterases, Nat. Rev. Drug Discov. 13 (4) (2014) 290–314.

[15] A. Lerner, P.M. Epstein, Cyclic nucleotide phosphodiesterases as targets for treatment of haematological malignancies, Biochem. J. 393 (Pt 1) (2006) 21–41.

[16] J. Colicelli, C. Birchmeier, T. Michaeli, K. O'Neill, M. Riggs, M. Wigler, Isolation and characterization of a mammalian gene encoding a high-affinity cAMP phosphodiesterase, Proc. Natl. Acad. Sci. U. S. A. 86 (10) (1989) 3599–3603.

[17] G. Bolger, T. Michaeli, T. Martins, T. St John, B. Steiner, L. Rodgers, M. Riggs, M. Wigler, K. Ferguson, A family of human phosphodiesterases homologous to the dunce learning and memory gene product of Drosophila melanogaster are potential targets for antidepressant drugs, Mol. Cell. Biol. 13 (10) (1993) 6558–6571.

[18] T. Michaeli, T.J. Bloom, T. Martins, K. Loughney, K. Ferguson, M. Riggs, L. Rodgers, J.A. Beavo, M. Wigler, Isolation and characterization of a previously undetected human cAMP phosphodiesterase by complementation of cAMP phosphodiesterase-deficient Saccharomyces cerevisiae, J. Biol. Chem. 268 (17) (1993) 12925–12932.

[19] R. Pillai, K. Kytle, A. Reyes, J. Colicelli, Use of a yeast expression system for the isolation and analysis of drug-resistant mutants of a mammalian phosphodiesterase, Proc. Natl. Acad. Sci. U. S. A. 90 (24) (1993) 11970–11974.

[20] R. Pillai, S.F. Staub, J. Colicelli, Mutational mapping of kinetic and pharmacological properties of a human cardiac cAMP phosphodiesterase, J. Biol. Chem. 269 (48) (1994) 30676–30681.

[21] F.D. Ivey, L. Wang, D. Demirbas, C. Allain, C.S. Hoffman, Development of a fission yeast-based high-throughput screen to identify chemical regulators of cAMP phosphodiesterases, J. Biomol. Screen. 13 (1) (2008) 62–71.

[22] C.S. Hoffman, F. Winston, Isolation and characterization of mutants constitutive for expression of the fbp1 gene of Schizosaccharomyces pombe, Genetics 124 (4) (1990) 807–816.

[23] C.S. Hoffman, F. Winston, Glucose repression of transcription of the Schizosaccharomyces pombe fbp1 gene occurs by a cAMP signaling pathway, Genes Dev. 5 (4) (1991) 561–571.

[24] D. Demirbas, O. Ceyhan, A.R. Wyman, C.S. Hoffman, A fission yeast-based platform for phosphodiesterase inhibitor HTSs and analyses of phosphodiesterase activity, Handbook of Experimental Pharmacology, vol. 204, 2011, pp. 135–149.

[25] D. Demirbas, O. Ceyhan, A.R. Wyman, F.D. Ivey, C. Allain, L. Wang, M.N. Sharuk, S.H. Francis, C.S. Hoffman, Use of a Schizosaccharomyces pombe PKA-repressible reporter to study cGMP metabolising phosphodiesterases, Cell. Signal. 23 (3) (2011) 594–601.

[26] M.A. Alaamery, A.R. Wyman, F.D. Ivey, C. Allain, D. Demirbas, L. Wang, O. Ceyhan, C.S. Hoffman, New classes of PDE7 inhibitors identified by a fission yeast-based HTS, J. Biomol. Screen. 15 (4) (2010) 359–367.

[27] A.S. de Medeiros, G. Kwak, J. Vanderhooft, S. Rivera, R. Gottlieb, C.S. Hoffman, Fission yeast-based high-throughput screens for PKA pathway inhibitors and activators, in: J.E. Hempel, C.H. Williams, C.C. Hong (Eds.), Chemical Biology: Methods and Protocols, Springer Humana Press, 2015(in press).

[28] A.S. de Medeiros, G. Kwak, J. Vanderhooft, S. Rivera, R. Gottlieb, C.S. Hoffman, Fission yeast-based high-throughput screens for PKA pathway inhibitors and activators, Methods Mol. Biol. 1263 (2015) 77–91.

[29] A.S. de Medeiros, A. Magee, K. Nelson, L. Friedberg, K. Trocka, C.S. Hoffman, Use of PKA-mediated phenotypes for genetic and small-molecule screens in Schizosaccharomyces pombe, Biochem. Soc. Trans. 41 (6) (2013) 1692–1695.

[30] H. Gutz, H. Heslot, U. Leupold, N. Loprieno, Schizosaccharomyces pombe, in: R.C. King (Ed.), Handbook of Genetics, Plenum Press, New York, 1974, pp. 395–446.

[31] L. Wang, K. Griffiths, Y.H. Zhang, F.D. Ivey, C.S. Hoffman, Schizosaccharomyces pombe adenylate cyclase suppressor mutations suggest a role for cAMP phosphodiesterase regulation in feedback control of glucose/cAMP signaling, Genetics 171 (2005) 1523–1533.

[32] R.T. Janoo, L.A. Neely, B.R. Braun, S.K. Whitehall, C.S. Hoffman, Transcriptional regulators of the Schizosaccharomyces pombe fbp1 gene include two redundant Tup1p-like corepressors and the CCAAT binding factor activation complex, Genetics 157 (3) (2001) 1205–1215.

[33] E. Apolinario, M. Nocero, M. Jin, C.S. Hoffman, Cloning and manipulation of the Schizosaccharomyces pombe his7+ gene as a new selectable marker for molecular genetic studies, Curr. Genet. 24 (6) (1993) 491–495.

[34] J. DeVoti, G. Seydoux, D. Beach, M. McLeod, Interaction between ran1$^+$ protein kinase and cAMP dependent protein kinase as negative regulators of fission yeast meiosis, EMBO J. 10 (12) (1991) 3759–3768.

[35] J. Buck, M.L. Sinclair, L. Schapal, M.J. Cann, L.R. Levin, Cytosolic adenylyl cyclase defines a unique signaling molecule in mammals, Proc. Natl. Acad. Sci. U. S. A. 96 (1) (1999) 79–84.

[36] J. Inglese, D.S. Auld, A. Jadhav, R.L. Johnson, A. Simeonov, A. Yasgar, W. Zheng, C.P. Austin, Quantitative high-throughput screening: a titration-based approach that efficiently identifies biological activities in large chemical libraries, Proc. Natl. Acad. Sci. U. S. A. 103 (31) (2006) 11473–11478.

[37] J.H. Zhang, T.D. Chung, K.R. Oldenburg, A simple statistical parameter for use in evaluation and validation of high throughput screening assays, J. Biomol. Screen. 4 (2) (1999) 67–73.

[38] K.Y. Beste, H. Burhenne, V. Kaever, J.P. Stasch, R. Seifert, Nucleotidyl cyclase activity of soluble guanylyl cyclase alpha1beta1, Biochemistry 51 (1) (2012) 194–204.

[39] S.L. Forsburg, Comparison of Schizosaccharomyces pombe expression systems, Nucleic Acids Res. 21 (12) (1993) 2955–2956.

[40] K. Hirota, T. Miyoshi, K. Kugou, C.S. Hoffman, T. Shibata, K. Ohta, Stepwise chromatin remodelling by a cascade of transcription initiation of non-coding RNAs, Nature 456 (7218) (2008) 130–134.

[41] S.A. Haney, J. Xu, S.Y. Lee, C.L. Ma, E. Duzic, J.R. Broach, J.P. Manfredi, Genetic selection in Saccharomyces of mutant mammalian adenylyl cyclases with elevated basal activities, Mol. Genet. Genom. 265 (6) (2001) 1120–1128.

[42] F.D. Ivey, C.S. Hoffman, Direct activation of fission yeast adenylate cyclase by the Gpa2 Gα of the glucose signaling pathway, Proc. Natl. Acad. Sci. U. S. A. 102 (17) (2005) 6108–6113.

[43] S. Landry, C.S. Hoffman, The git5 Gβ and git11 Gγ form an atypical Gβγ dimer acting in the fission yeast glucose/cAMP pathway, Genetics 157 (3) (2001) 1159–1168.

[44] S. Landry, M.T. Pettit, E. Apolinario, C.S. Hoffman, The fission yeast git5 gene encodes a Gβ subunit required for glucose-triggered adenylate cyclase activation, Genetics 154 (4) (2000) 1463–1471.

[45] R.M. Welton, C.S. Hoffman, Glucose monitoring in fission yeast via the gpa2 Gα, the git5 Gβ, and the git3 putative glucose receptor, Genetics 156 (2000) 513–521.

[46] F.D. Ivey, F.X. Taglia, F. Yang, M.M. Lander, D.A. Kelly, C.S. Hoffman, Activated alleles of the Schizosaccharomyces pombe gpa2+ Galpha gene identify residues involved in GDP-GTP exchange, Eukaryot. Cell 9 (4) (2010) 626–633.

[47] K. Petrovic, M. Pfeifer, C.N. Parker, S. Schuierer, J. Tallarico, D. Hoepfner, N.R. Movva, G. Scheel, S.B. Helliwell, Two low complexity ultra-high throughput methods to identify diverse chemically bioactive molecules using Saccharomyces cerevisiae, Microbiol. Res. 199 (2017) 10–18.

[48] J.L. Norcliffe, J.G. Mina, E. Alvarez, J. Cantizani, F. de Dios-Anton, G. Colmenarejo, S.G. Valle, M. Marco, J.M. Fiandor, J.J. Martin, P.G. Steel, P.W. Denny, Identifying inhibitors of the Leishmania inositol phosphorylceramide synthase with anti-protozoal activity using a yeast-based assay and ultra-high throughput screening platform, Sci. Rep. 8 (1) (2018) 3938.

[49] Y. Zhu, S. Fan, N. Wang, X. Chen, Y. Yang, Y. Lu, Q. Chen, J. Zheng, X. Liu, NADPH oxidase 2 inhibitor diphenyleneiodonium enhances ROS-independent bacterial phagocytosis in murine macrophages via activation of the calcium-mediated p38 MAPK signaling pathway, Am. J. Transl. Res. 9 (7) (2017) 3422–3432.

[50] D.J. Morre, Preferential inhibition of the plasma membrane NADH oxidase (NOX) activity by diphenyleneiodonium chloride with NADPH as donor, Antioxid. Redox Signal. 4 (1) (2002) 207–212.

[51] S. Muzaffar, J.Y. Jeremy, G.D. Angelini, K. Stuart-Smith, N. Shukla, Role of the endothelium and nitric oxide synthases in modulating superoxide formation induced by endotoxin and cytokines in porcine pulmonary arteries, Thorax 58 (7) (2003) 598–604.

[52] B.J. Michell, Z. Chen, T. Tiganis, D. Stapleton, F. Katsis, D.A. Power, A.T. Sim, B.E. Kemp, Coordinated control of endothelial nitric-oxide synthase phosphorylation by protein kinase C and the cAMP-dependent protein kinase, J. Biol. Chem. 276 (21) (2001) 17625–17628.

[53] C. Ye, Z. Zhang, Z. Wang, Q. Hua, R. Zhang, X. Xie, Identification of a novel small-molecule agonist for human G protein-coupled receptor 3, J. Pharmacol. Exp. Ther. 349 (3) (2014) 437–443.